

Lignocellulolytic microbiomes orchestrating degradation cascades in the rumen of dairy cattle and their diet-influenced key degradation phases

2024 Volume 1, Article number: e002

<https://doi.org/10.48130/animadv-0024-0002>

Received: 20 August 2024

Revised: 14 September 2024

Accepted: 18 September 2024

Published online: 21 October 2024

Limei Lin^{1,2}, Huiting Ma^{1,2}, Jiawei Zhang^{1,2}, Huisheng Yang^{1,2}, Jiyou Zhang^{1,2}, Zheng Lai^{1,2}, Weibiao Qi^{1,2}, Fei Xie^{1,2}, Weiyun Zhu^{1,2} and Shengyong Mao^{1,2*}

¹Ruminant Nutrition and Feed Engineering Technology Research Center, College of Animal Science and Technology, Nanjing Agricultural University, Nanjing 210095, China

²Laboratory of Gastrointestinal Microbiology, Jiangsu Key Laboratory of Gastrointestinal Nutrition and Animal Health, National Center for International Research on Animal Gut Nutrition, College of Animal Science and Technology, Nanjing Agricultural University, Nanjing 210095, China

* Corresponding author, E-mail: maoshengyong@njau.edu.cn

Abstract

Dairy cattle (*Bos taurus*) can convert lignocellulosic biomass into milk efficiently *via* their rumen symbiotic microbiota. However, the mechanisms by which the rumen microbiota of cows mediate the degradation cascades of lignocellulose and the specific stages primarily affected by dietary interventions remain unclear. Herein, 244 rumen metagenome samples from Holstein cows were used, identifying 1353 high-quality microbial metagenome-assembled genomes (MAGs) responsible for the degradation cascades of lignocellulose. It was revealed that *Fibrobacter* spp. and *Ruminococcus* spp. exhibited numerous endo-/exo-glucanases with accessory non-catalytic multi-carbohydrate binding modules for highly efficient cellulolytic abilities. *Prevotella* spp. and *Cryptobacteroides* spp. developed diverse polysaccharide utilization loci (PULs) to tackle the main and side chains of hemicellulose, particularly acetylxyylan esterase-contained PULs. Notably, novel and potential lignocellulolytic microbiomes were identified in the rumen of dairy cattle, such as *Hallerella* spp., *Sodaliphilus* spp., and *Mageeibacillus* spp. Through *in vivo* diet intervention and *in sacco* rumen incubation, it was discovered that high-grain diets primarily affected *Prevotella* spp., leading to a reduction in the initial degradation of amorphous regions in lignocellulose. Therefore, the present findings systematically illustrate the orchestrated enzymatic strategies of the cow rumen microbiota for the degradation cascades of lignocellulose, contributing to the dietary regulation of dairy cattle.

Citation: Lin L, Ma H, Zhang J, Yang H, Zhang J, et al. 2024. Lignocellulolytic microbiomes orchestrating degradation cascades in the rumen of dairy cattle and their diet-influenced key degradation phases. *Animal Advances* 1: e002 <https://doi.org/10.48130/animadv-0024-0002>

Introduction

Lignocellulose is a complex biopolymer composed primarily of cellulose, hemicellulose, and lignin, displaying significant resistance to hydrolysis^[1,2]. Deriving nutritional value from lignocellulose is challenging due to the highly resistant crystalline cellulose regions and the lignin coating that encapsulates the polysaccharide network^[3]. Mammals typically lack the enzymes to efficiently break down complex lignocellulosic biomass, relying heavily on microbes residing in the digestive tract to perform this function^[4]. Especially in ruminants, the symbiotic microbiota process the efficient conversion of lignocellulose into high-nutritious foods. For decades, studies have shown that lignocellulolytic degradation is primarily conducted by the rumen microbial community sequentially and synergistically, and the rumen microbiota has thus been employed as a model system to discover the enzyme repertoires for lignocellulose depolymerization^[5,6]. Despite the extensive research on lignocellulose degradation in the rumen, the specific diversity of the rumen microbiota responsible for each stage of the degradation cascades of various lignocellulosic components remains to be elucidated. Understanding the microbial diversity and substrate specificity is crucial for developing targeted strategies to enhance the efficiency of lignocellulose degradation and harness its full potential as a sustainable resource.

Microorganisms employ diverse enzymatic strategies for lignocellulose degradation. One strategy involves cellulosomes, multienzyme

assemblies efficiently degrading lignocellulose^[7,8]. These assemblies consist of cell surface-anchored scaffolding proteins with cohesion and dockerin domains, binding multiple carbohydrate-active enzymes (CAZymes, such as glycoside hydrolases)^[9]. Another strategy, encoded by specific polysaccharide utilization loci (PULs), exhibits somewhat 'selfish' behavior by transporting depolymerized products of complex polysaccharides into microbial cells, limiting sugar release into the environment and access for other scavenging populations^[10,11]. Additionally, non-catalytic module carbohydrate-binding modules (CBMs) with various substrate-binding capabilities play an important role in lignocellulose degradation^[12,13]. Despite the identification of numerous lignocellulose-degrading enzymes at the molecular level, the enzymatic strategies employed by ruminal microbiota for the degradation cascades of lignocellulosic components remain limited.

The lignocellulose degradation process involves fiber colonization, amorphous region degradation, specific bacterial population increase, and crystalline region degradation^[14]. Different microorganisms sequentially dominate these phases, driven by niche partitioning and microbial interactions^[14]. Previous studies have reported that the physicochemical properties of feed can be the primary factors that determine microbial colonization and digestion in the rumen^[8,15,16]. In particular, the diversity and composition of microbiota in the rumen differ between forage-fed and grain-fed animals^[4], implying that their microbial colonization and digestion in lignocellulosic biomass is

different. Despite the recognized influence of high-grain diets on altering microbial communities and reducing lignocellulose degradation, it remains unclear which phase of degradation cascades is mainly affected and how this reduction occurs.

Here, 244 rumen metagenome samples were analyzed from Holstein cows, constructing 5034 microbial metagenome-assembled genomes (MAGs). These MAGs underwent functional comparison, serving as a base for subsequent experiments, including *in vivo* high-grain diet interventions and *in sacco* rumen incubation. This comprehensive approach provided insights into lignocellulose degradation from both spatial and temporal perspectives. The integrated datasets allowed (1) identification of the diversity of lignocellulolytic microbiomes (LMs) and their diverse enzymatic strategies for specific lignocellulosic components during the degradation cascades, (2) elucidate the primary lignocellulosic components affected by high-grain diets and identify the key microbial players involved, and (3) clarify which stage of the lignocellulolytic cascades is predominantly influenced by high-grain diets and identify the primary microbial contributors to these effects. Based on a vast array of uncultured microbial genomes, the findings provide a more in-depth understanding of the lignocellulose degradation cascades of rumen microbiota, particularly in relation to diet, offering insights for promoting the efficient conversion of low-quality lignocellulosic biomass into highly nutritious milk in dairy cattle in the future.

Materials and methods

Animal experiment design and sample collection

Twelve lactating Holstein cows with rumen fistulas, weighing 651 ± 54 kg, were housed in tie stalls for a one-month experiment^[4]. Before the animal trial, all cows were fed a diet with a forage-to-grain ratio of 6:4 for one week. After this preparation period, six cows were fed on a high-forage diet with a forage-to-grain ratio of 6:4 on a dry matter (DM) basis (CON group), whereas the six other cows were fed a high-grain diet with a forage-to-grain ratio of 4:6 on a DM basis (HG group; [Supplementary Table S7](#)). The feeding trial lasted for 21 d, and the animals were fed *ad libitum* twice a day (07:00 and 19:00). The feed and fecal samples were collected at 07:00 and 19:00 for three consecutive days before the cows were slaughtered. The feed and fecal samples were processed for chemical composition analysis, including dry matter (DM), neutral detergent fiber (NDF), and acid detergent fiber (ADF)^[17]. To assess the apparent digestibility of DM, NDF, and ADF, acid insoluble ash (AIA) was used as an internal marker^[18]. After the experiment, all cows were slaughtered to collect rumen contents and stored at -80 °C. The rumen contents were further used for DNA extraction.

Ruminal *in situ* incubations and sample collection

Six lactating rumen-fistulated Holstein cows (CON group: $n = 3$; HG group: $n = 3$) were selected for *in sacco* rumen incubation. The *Leymus chinensis* materials were dried and cut into 2.5 mm pieces. The pieces were weighed and 4 g of them were placed in each heat-sealed nylon bag (bag size: 8 cm \times 12 cm; pore size: 300 μ m). A total of 96 heat-sealed bags, 16 per cows, were simultaneously placed into each rumen before morning feeding. After 0.5, 2, 4, 6, 8, 12, 24, and 36 h of incubation, two nylon bags were retrieved at each time point from each cow's rumen, washed three times with distilled water to eliminate liquid-borne and loosely attached microbes, and then squeezed to remove excess water. The incubated *Leymus chinensis* samples in nylon bags were transferred to the laboratory in liquid nitrogen. One replicate was used for subsequent DNA extraction, while the other was subjected to chemical composition analysis, including DM, NDF, and ADF^[17]. The *Leymus chinensis* samples were also stored for chemical composition analysis.

DNA extraction and metagenomic sequencing

The DNA from the incubated *Leymus chinensis* samples (including 0.5, 2, 4, 6, 8, 12, 24, and 36 h of rumen incubation) was extracted using a microbead stirrer (BioSpec Products, Inc., Bartlesville, OK, USA)^[19] and the E.Z.N.A.® Stool DNA Kit (Omega Bio-tek, Norcross, GA, USA) according to the manufacturer's protocols. The quality and quantity of the extracted DNA were determined using the Nanodrop ND-1000 (Thermo Scientific, Wilmington, USA), and the integrity of the DNA was evaluated through electrophoresis on 0.8% agarose gels. The high-quality DNA samples were then stored at -80 °C until further processing.

16S rRNA gene sequencing

The extracted high-quality DNA was further used for 16S rRNA gene sequencing. The V3 and V4 regions of the gene were amplified using universal primers (341F: 5'-CCTAYGGGRBGCASCAG-3', 806R: 5'-GGACTACNNGGTATCTAAT-3'), with a 6 bp barcode unique to each sequence. The Illumina MiSeq platform was used for sequencing, and the barcodes and sequencing primers were removed for data processing. After removing low-quality reads, the remained paired-end reads were merged using FLASH^[20] (v.1.2.7). The sequences were further screened to remove chimeras and dereplication by the procedure of 'removeBimeraDenovo', and ASV feature tables were constructed using the DADA2^[21] (v.1.18) plug-in in QIIME 2^[22] (v.2021.08). The ASVs were taxonomically assigned against the SILVA v.138 database^[23] using the naive Bayes classifier^[24].

Fiber-adherent rumen metagenomic sequencing

The microbial DNA extracted from 18 ruminal incubated *Leymus chinensis* samples (0.5, 8, and 36 h) was used for metagenomic sequencing. For each sample, the high-quality DNA samples were utilized to generate a metagenomic library with an insert size of 350 bp following the manufacturer's instructions for the TruSeq DNA PCR-Free Library Preparation Kit (Illumina, San Diego, CA, USA). The resulting library was sequenced on the Illumina NovaSeq platform to obtain the sequence data.

Metagenome assembly and binning

The Illumina data from 18 fiber-adherent rumen metagenome samples and 226 published ruminal metagenome samples from dairy cattle was processed^[4-6,25-33]. First, quality control was performed on the data using Fastp^[34] (v.0.20.1) to trim adapters, then the host (*Bos taurus*, GCA_002263795.2), food was removed, and human sequences (*Homo sapiens*, GCA_000001405.28) by using BWA-MEM^[35] (v.0.7.17) according to a previous study^[4]. The reference genome sets of plants in feed included wheat (*Triticum aestivum*, GCA_002220415.3), medicago (*Medicago truncatula*, GCA_000219495.2), rice (*Oryza sativa*, GCF_000005425.2), maize (*Zea mays*, GCA_003185045.1 and GCA_000005005.6), and soybean (*Glycine max*, GCA_000004515.4). MEGAHIT^[36] (v.1.2.9) was applied to assemble the high-quality reads from each sample (parameter: --min-contig-len 500 --presets meta-large). The remaining high-quality contigs were binned into genomes by three different approaches, including MaxBin^[37] (v.2.2.4), MetaBAT2^[35] (v.2.11.1), and CONCOCT^[38] (v.0.4.0) with default parameters. The obtained genomes were integrated using the bin refinement module of metaWRAP^[39] (v.1.3). Prokaryotic metagenome-assembled genomes (MAGs) were evaluated for completeness and contamination using CheckM^[40] (v.1.0.7). Among them, 5,034 rumen microbial MAGs exhibited completeness over 50% and contamination below 10%. The non-redundant 3,808 MAGs were remained, with a dereplication threshold of 99% average nucleotide identity by using dRep^[41] (v3.4.0). After filtering for completeness > 80% and contamination < 10%, 1374 MAGs were obtained to predict ORFs by Prokka^[42] (v.1.14.6). The estimated genome size of 5,034 MAGs was corrected based on completeness and contamination using the algorithm from Nayfach et al.^[43].

Taxonomic and functional annotation

All 1374 high-quality genomes were subjected to annotation using GTDB-Tk^[44] (v.0.1.6) based on the Genome Taxonomy Database. Subsequently, a maximum-likelihood phylogenomic tree was constructed using PhyloPhlan^[45] (v.1.0) and visualized using iTol^[46] (v.4.3.1). The carbohydrate-active enzyme (CAZyme) profiles of each MAG were annotated using dbCAN2^[47]. The assignment of dockerin domains of each MAG was predicted based on the hidden Markov model (HMM) using HMMER^[48] (v.3.2.1), according to the CAZyme database^[49]. Putative lignocellulolytic microbiomes (LMs) as genomes containing any of the CAZyme families capable of lignocellulose degradation were identified, including GH5, GH51, GH48, GH9, GH44, GH74, GH124, GH148, GH45, GH8, GH10, GH2, GH3, GH1, GH116, GH43, GH30, GH98, GH11, GH141, GH39, GH54, GH120, CE1, GH67, CE3, CE5, CE7, GH159, GH4, GH110, GH26, GH113, GH164, CE2, CE4, GH27, GH31, GH36, GH57, CE6, CE12, GH97, CE15, AA1, AA3, AA4, AA6, and AA7. The polysaccharide utilization loci (PUL) of all 1374 MAGs were predicted following PULpy^[50] (v.1.0) pipeline. Finally, all 1353 LM-MAGs were employed as a genomic database to assign metagenomic samples from the 12 dairy cattle rumen and 18 fiber-adherent rumen by using CoverM (v.0.6.1; <https://github.com/wwood/CoverM>) (parameter: --min-read-percent-identity 0.95 --min-read-aligned-percent 0.75 --trim-min 0.10 --trim-max 0.90 -m tpm --proper-pairs-only). Subsequently, the transcripts per million (TPM) calculation process was employed to quantify the abundance levels of each genome in these samples.

Statistical analysis

To compare the feed apparent digestibility of DM, NDF, and ADF between the CON and HG groups, a *t*-test model was used. For the digestibility of DM, NDF, and ADF in the incubated *Leymus chinensis* material, a *t*-test analysis was performed at each time point to compare between the CON and HG groups. To identify the differences between the two groups at the ASV level, Principal Coordinates Analysis (PCoA) based on the Bray-Curtis distance was performed and an ANOSIM test conducted with 9999 permutations using the R vegan package (v.2.6-4). The changes of ASVs between the CON and HG groups among the eight time points during rumen incubation were analyzed using the R packages indicspecies (v.1.7.12) and edgeR (v.3.36.0). Weighted Correlation Network Analysis (WGCNA, v.1.71) was employed to construct co-occurrence modules based on the ASVs with significantly changed abundance, with MEDissThres set to 0.2. Additionally, a Wilcoxon rank-sum test was performed to compare the abundance of MAGs between the CON and HG groups. Relationships between the changes and the number of genes encoding lignocellulolytic CAZymes of *Prevotella*-affiliated MAGs were based on Spearman.

Results

Heterogeneous microbial consortium for lignocellulose degradation from dairy cattle rumen

To establish a potent lignocellulolytic consortium in the rumen of dairy cattle, 244 metagenome samples from Holstein cows were used to construct 5034 rumen microbial MAGs, which had completeness of over 50% and contamination below 10% (Supplementary Fig. S1a; Supplementary Tables S1 & S2). The non-redundant 3808 MAGs with a dereplication threshold of 99% average nucleotide identity were observed. Within this subset, 1374 high-quality MAGs were identified with > 80% completeness and < 10% contamination, which had a mean completeness of 89.51% (\pm 0.15%) and a mean contamination of 3.04% (\pm 0.06%) (Supplementary Fig. S1b; Supplementary Table S3). For taxonomic profiling, 100%, 99.56%, and 81.88% of MAGs were classified into microbes at the phylum, genus, and species levels, respectively (Supplementary Table S3). The genomic repertoire of the rumen microbiome

encompassed 23 phyla, 86 families, and 268 genera in dairy cattle (Supplementary Table S3). The integrated microbial MAGs from dairy cattle rumen are more representative than those previously reported^[4].

In the CAZyme analysis, 1353 high-quality MAGs (98.47%) were identified to be involved in the degradation process of lignocellulose, including cellulose, hemicellulose, and lignin (Fig. 1a, Supplementary Table S4). This ability enables cows to efficiently convert complex and recalcitrant plant biomass into valuable nutrients. All 1353 MAGs represented LMs consisting of 23 phyla, with the distribution including Bacteroidota (519), Firmicutes_A (510), Firmicutes (90), Spirochaetota (58), Firmicutes_C (48), Proteobacteria (42), Methanobacteriota (19), Actinobacteriota (18), Fibrobacterota (10), Elusimicrobiota (9), Cyanobacteria (8), and Verrucomicrobiota (8). These LMs contained 35,043 genes encoding lignocellulolytic CAZymes, covering 49 distinct families (Supplementary Table S4). The number of genes encoding lignocellulolytic CAZymes in LMs was strongly positively correlated with their genome size (Mantel test, $R = 0.661$, $p < 0.001$; Fig. 1b), suggesting that the lignocellulose degrading ability is closely related to other microbial functions. Certain LM-MAGs, particularly those belonging to the Verrucomicrobiota, Bacteroidota, and Fibrobacterota phyla exhibited the most extensive and diverse repertoire of CAZymes for the lignocellulose degradation (Fig. 1a, c). Members of the Fibrobacterota phylum demonstrated a more varied repertoire of CAZyme families for lignocellulose degradation compared to those in the Actinobacteriota phylum. Additionally, Firmicutes_A exhibited a less diverse repertoire of CAZymes for lignocellulose degradation compared to the Bacteroidota phylum. Furthermore, the Proteobacteria phylum had the lowest number of genes and families encoding lignocellulolytic CAZymes. These observations imply that the diversity and redundancy of lignocellulolytic CAZymes within microbial consortia may contribute to variations in the breakdown and utilization of plant fibers.

Deciphering lignocellulolytic consortia and their enzymatic strategies involved in degradation cascades of various lignocellulosic components

Lignocellulose is a complex and recalcitrant structure composed primarily of cellulose, hemicellulose, and lignin, which provide plants with rigidity and durability. For cellulose, GH5 was identified as the most abundant cellulolytic enzyme in rumen LMs, particularly within the Bacteroidota phylum (Fig. 2a). Members of *Fibrobacter* and *Ruminococcus* (e.g., *Ruminococcus flavefaciens*) had the largest number of CAZyme genes coding endo- and exoglucanases (primarily GH5 and GH9; Fig. 2b). Therefore, these microbial populations play a significant role in cellulose degradation by primarily attacking cellulose fibrils at the amorphous regions, followed by cutting at the crystalline regions from both the reducing and non-reducing ends. *Ruminococcus* MAGs were found to encode GH48, enabling them to target both amorphous and crystalline cellulose (Fig. 2b). Compared with *Ruminococcus* spp., *Fibrobacter* spp. exhibited a more diverse array of CAZyme families to attack amorphous regions of cellulose by encoding endoglucanases GH45 and GH8 (Fig. 2b). In addition, the enzymes involved in lignocellulose degradation often feature a CBM attached to the catalytic domain^[12]. Notably, *Ruminococcus* spp. (25) and *Fibrobacter* spp. (23) displayed the highest counts of CBM-containing enzymes, many of which had N-terminal signal peptides (Supplementary Table S5). This highlights the abundance of secreted or periplasmic multi-domain enzymes in these populations, which are highly effective in lignocellulose degradation. *Ruminococcus* spp., in particular, had adapted to produce complex proteins with multiple catalytic domains, often accompanied by one or two CBMs to target amorphous cellulose and hemicellulose. This was particularly evident in numerous PULs (CBM4 + GH9; Fig. 3). In contrast, certain proteins identified in *Fibrobacter* spp. contained three

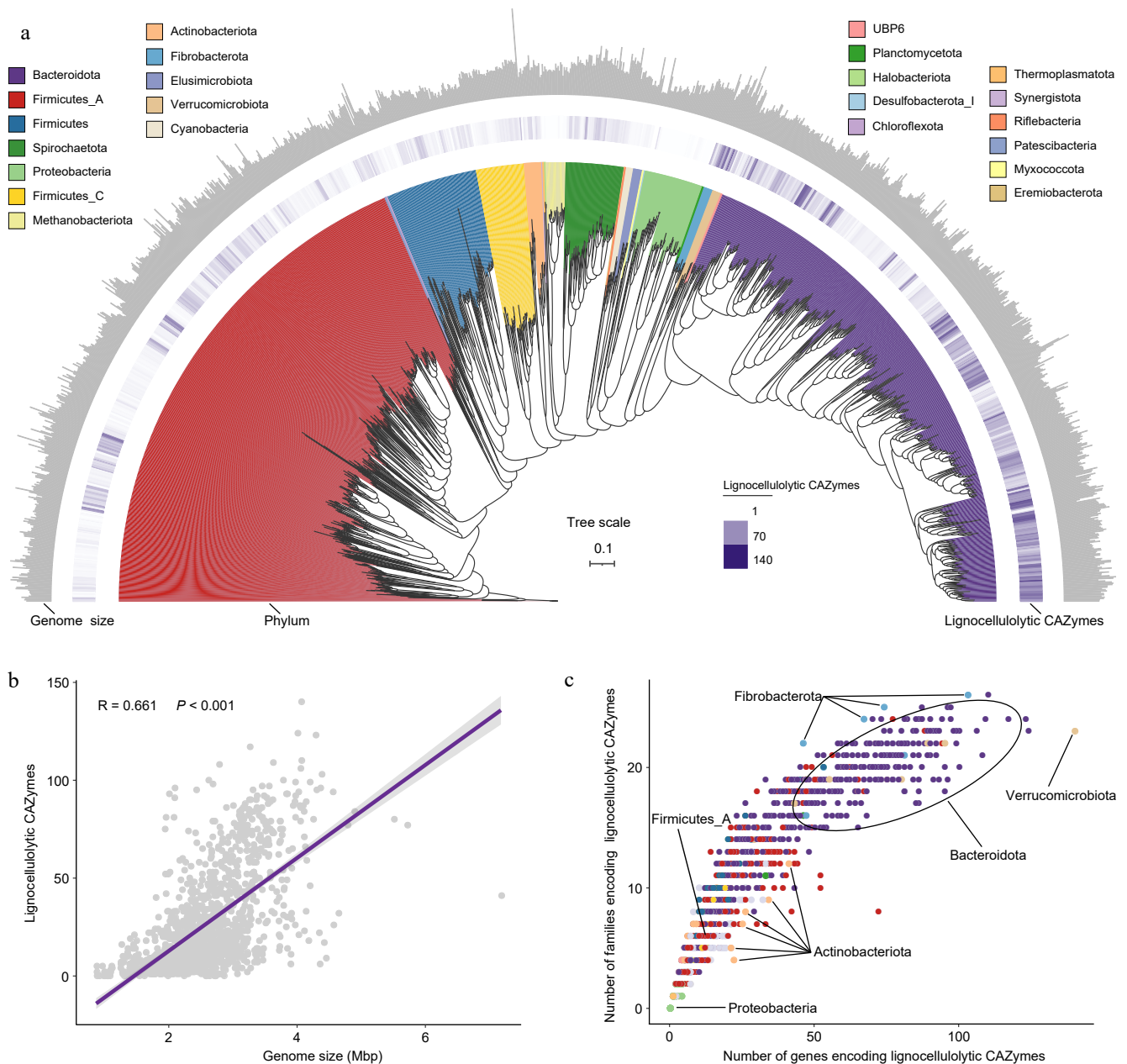


Fig. 1 The CAZyme profiles in lignocellulolytic microbiomes (LMs) from dairy cattle rumen. (a) Phylogenetic tree of 1353 microbial metagenome-assembled genomes (MAGs) coding lignocellulolytic CAZymes. The maximum-likelihood tree is constructed using PhyloPhAn. Branches are shaded with color to highlight phylum-level affiliations. The inside layer of the heat map represents number of genes encoding lignocellulolytic CAZymes of each LM-MAG. The outside layer of the bar graph represents the genome size of each LM-MAG. (b) The correlation between number of genes encoding lignocellulolytic CAZymes and genome size of LM-MAGs. (c) Number of degradative CAZymes in distinct families in each LM-MAG. Genomes are colored by phylum.

tandemly arranged CBMs and one GH domain (CBM11 + CBM11 + CBM11 + GH51) to adhere cellulosic biomass (Fig. 3). The most significant disparity between *Ruminococcus* and *Fibrobacter* was that *Ruminococcus* had a multitude of dockerin and cohesion domains, whereas *Fibrobacter* lacked such domains, implying that *Ruminococcus* possesses the ability to produce cellulosomes for fiber digestion^[51] (Supplementary Table S3). Additionally, no genes encoding lytic polysaccharide monoxygenases (LPMOs) targeting cellulosic crystalline substrates were found in the LMs of dairy cattle rumen. For β -glucosidases, members of the Bacteroidales order were the major agents of hydrolyzing glucose dimers into glucose (e.g., GH2 and GH3; Supplementary Table S4).

For hemicellulose degradation, the predominant CAZyme family

identified within LMs was GH43, with a notable presence in the Bacteroidota phylum (Fig. 2a). Within the Bacteroidota population, the distribution of lignocellulolytic CAZymes exhibited a similar pattern (Fig. 2a), suggesting a considerable degree of conservation in their enzymatic systems. Members of the Bacteroidota phylum, primarily *Prevotella* spp. and *Cryptobacteroides* spp., were found to encode enzymes such as endoxylanase, β -xylosidase, and de-branching activities (primarily GH43, GH2, GH3, and CE1; Fig. 2b). Furthermore, it was observed that *Prevotella* spp. and *Cryptobacteroides* spp. encoded a substantial number of PULs to handle the chemical and structural complexity of hemicelluloses such as xylose, arabinose, galactose, mannose, and ferulic acid (Supplementary Table S6). It is noteworthy that most of the *Prevotella* and *Cryptobacteroides* MAGs

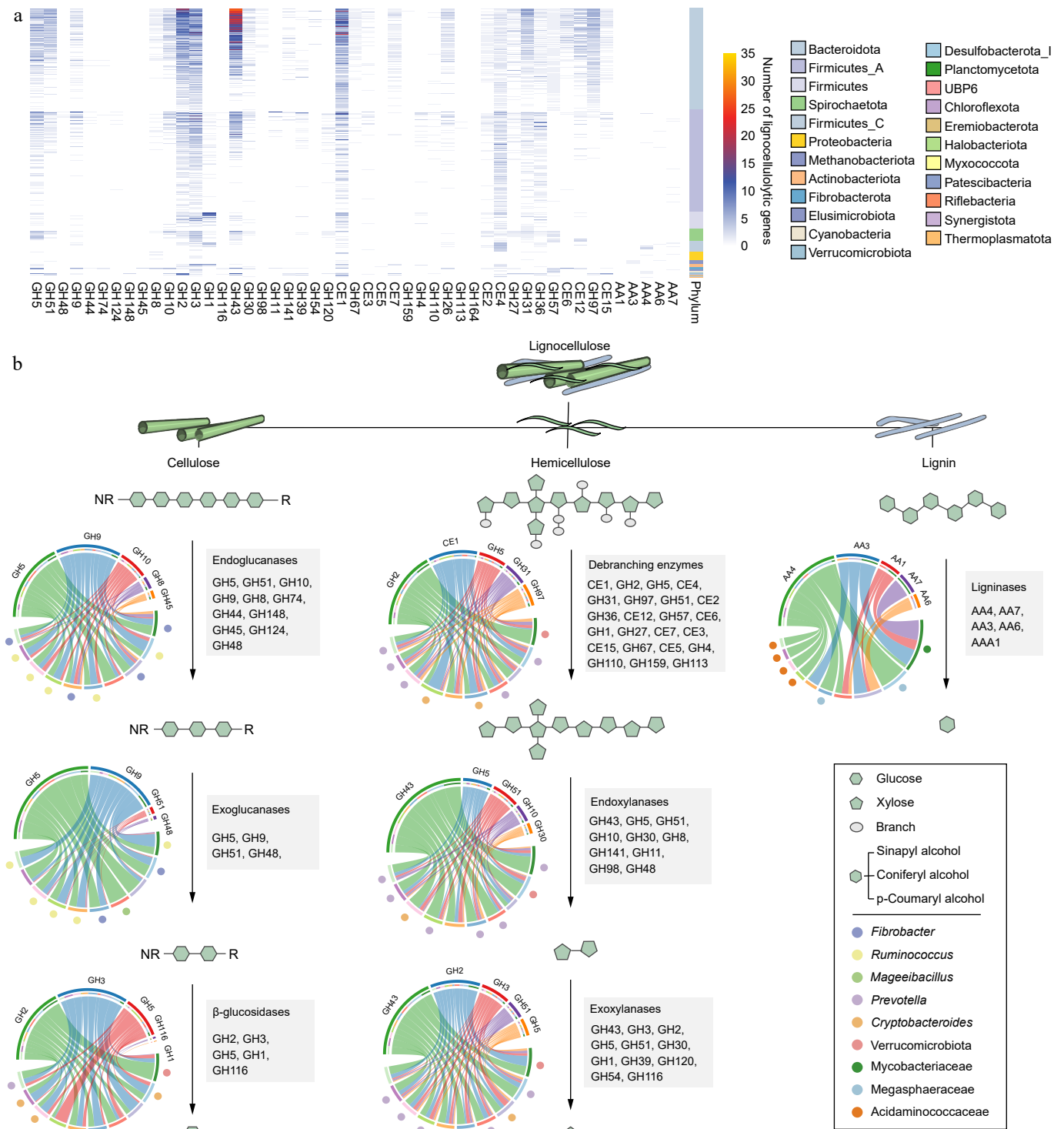


Fig. 2 The distribution and diversity of lignocellulolytic microbiomes (LMs) from dairy cattle rumen. (a) Distribution of lignocellulolytic CAZymes (GH, glycoside hydrolases; CE, carbohydrate esterases; AA, Auxiliary Activities) in LM-MAGs. Genomes are colored by phylum. (b) Cooperative model of cellulases, hemicellulases, and ligninases in lignocellulose degradation in the LM-MAGs. Chord Diagram represent the top families of lignocellulolytic CAZymes contributed by ruminal LM-MAGs. The detailed information regarding LMs involved in the degradation process of lignocellulose, including cellulose, hemicellulose, and lignin, can be found in Table S4.

contained acetylxylan esterase-containing PULs (Fig. 3), facilitating the breakdown of the xylan backbone. These results indicate that *Prevotella* spp. and *Cryptobacteroides* spp. have developed PULs to address the challenges posed by complex and diverse hemicelluloses, which are subsequently transported into the cells for their utilization.

Despite the presence of diverse CAZyme repertoires, only a few

enzymes involved in lignin breakdown were identified in the rumen microbiome of dairy cattle (Fig. 2a). Specifically, only 135 MAGs (9.82%) encoded AA1, AA3, AA4, AA6, or AA7 enzymes involved in lignin modification and degradation, primarily belonging to the classes Clostridia (47 MAGs), Negativicutes (26 MAGs), and Methanobacteria (17 MAGs; Supplementary Table S4). The AA family with the

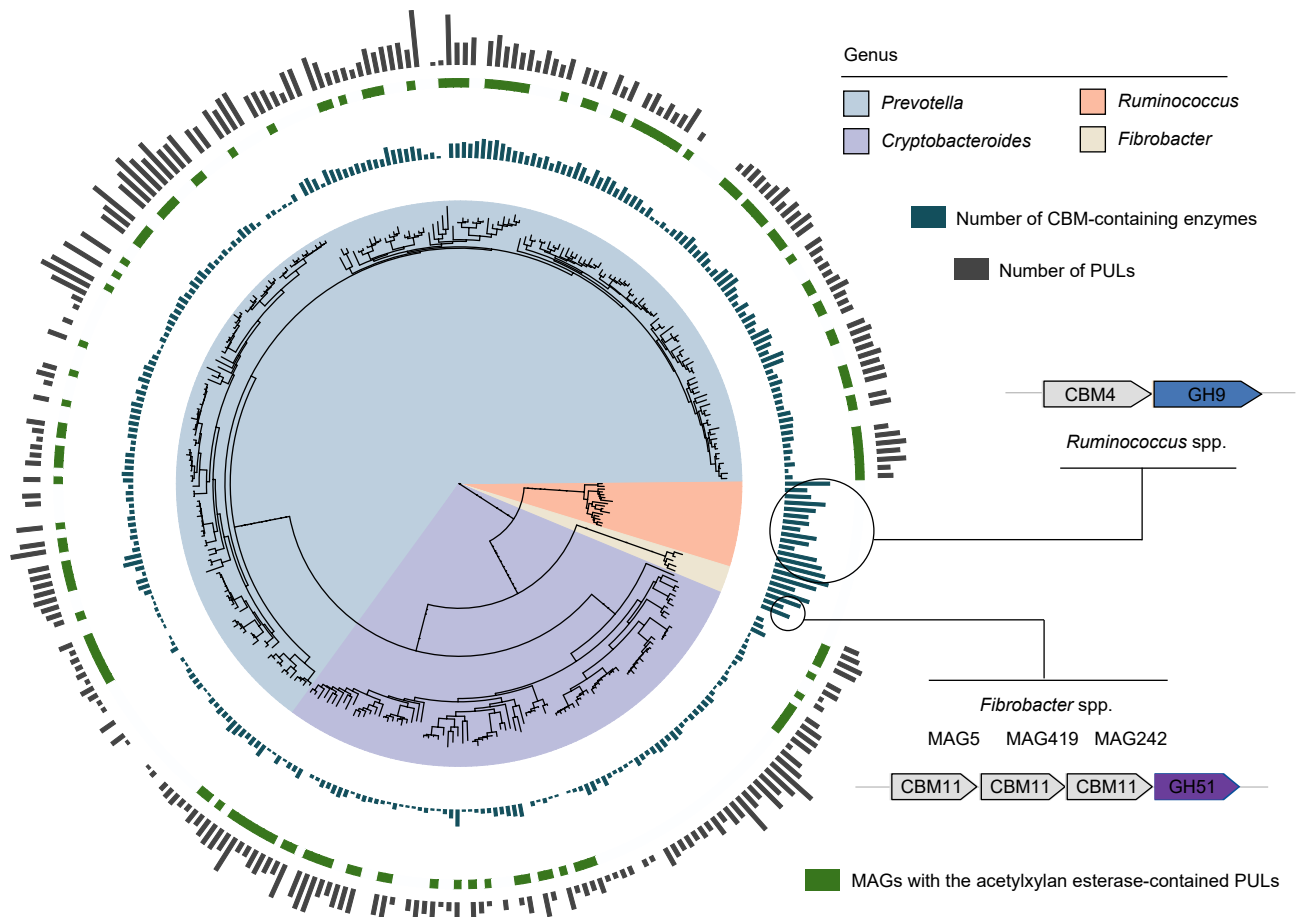


Fig. 3 Different lignocellulose degradation strategies used by taxa present in the dairy cattle rumen. Phylogenetic tree of lignocellulolytic microbiomes (LMs) belonged to genera *Prevotella*, *Cryptobacteroides*, *Ruminococcus*, and *Fibrobacter*. The maximum-likelihood tree is constructed using PhyloPhlAn. The background of branches is shaded with color to highlight these four taxa. The inside layer of the bar graph represents number of CBM-containing enzymes. The green color represents the specific MAGs with the acetylxylan esterase-contained PULs. The outside layer of the bar graph represents the number of polysaccharide utilization loci (PULs) encoded by the targeted MAGs.

highest number of genes was vanillyl-alcohol oxidase AA4 (consisting of 89 genes) used for lignin degradation (Fig. 2a). In contrast, only eight genes coding for laccase AA1 were identified for lignin modification (Fig. 2a). These findings suggest that the rumen microbiota in dairy cattle has a limited capacity to degrade lignin from plant biomass.

Novel consortium involved in degradation cascades of various lignocellulosic components

Among the 1353 LM-MAGs identified, some members of the Fibrobacteraceae family, such as *Hallerella* spp., were isolated from pig intestines in 2020^[52] and had not been previously reported in ruminants. Genome annotation against the CAZy database revealed that four *Hallerella*-affiliated MAGs possessed a large number of cellulases belonging to the families GH5 and GH9, but only a few of these cellulases were found to be fused with CBM domains (Supplementary Tables S4 & S5). This suggests that *Hallerella* spp. may have the potential to utilize cellulose as a carbohydrate substrate^[52]. Additionally, *Mageeibacillus* spp., previously isolated from the human vagina, contained the highest number of endo- and exoglucanases belonging to the GH5 family, as well as dockerin (Fig. 2b; Supplementary Table S3). *Sodaliophilus* is a recently described genus, with its type species *S. pleomorphus*, initially isolated from pig feces^[52]. It is noteworthy that it was identified that 32 MAGs could be annotated to *Sodaliophilus* (including *S. pleomorphus*) in the dairy cattle rumen, which had the largest number of dockerins and was enriched in hemicellulose and cellulose-degrading enzymes

(Supplementary Table S3). However, *Sodaliophilus* did not contain any cohesion domains, suggesting that the numerous non-cellulosomal dockerins may have other functions^[7]. Analysis of PULs revealed that each of the *Sodaliophilus*-affiliated MAGs contained seven PULs, with *S. pleomorphus* having more than ten PULs (Supplementary Table S6). Therefore, we hypothesize that *Sodaliophilus* is a potential lignocellulose degrader in the rumen. Overall, the identification of potential lignocellulolytic consortia may open new opportunities for enhancing the degradation of plant fibers in dairy cattle production.

Selective reduction of hemicellulose degradation in the rumen by high-grain diets

The 1353 LM-MAGs were further employed as a genomic database to assign metagenomic samples from the CON and HG groups in dairy cattle rumen to explore the substantial alterations in microbial communities and enzyme abundances during the degradation processes of cellulose, hemicellulose, and lignin affected by high-grain diets (Fig. 4a; Supplementary Table S7). In the depolymerization phase of celluloses, genomes containing endoglucanases, particularly from the genera *Ruminococcus* and *Hallerella* exhibited a significant increase in abundance under high-grain diet conditions (Wilcoxon rank-sum test, $p < 0.05$; Fig. 4b & Supplementary Table S8). Meanwhile, the grain-based diet increased the abundance of endo- β -1,4-glucanase GH124 (Fig. 4b). Therefore, *Ruminococcus* spp. and *Hallerella* spp. emerged as the primary agents targeting cellulose fibrils at the amorphous regions during high-grain diet feeding conditions. In the subsequent cellulose degradation

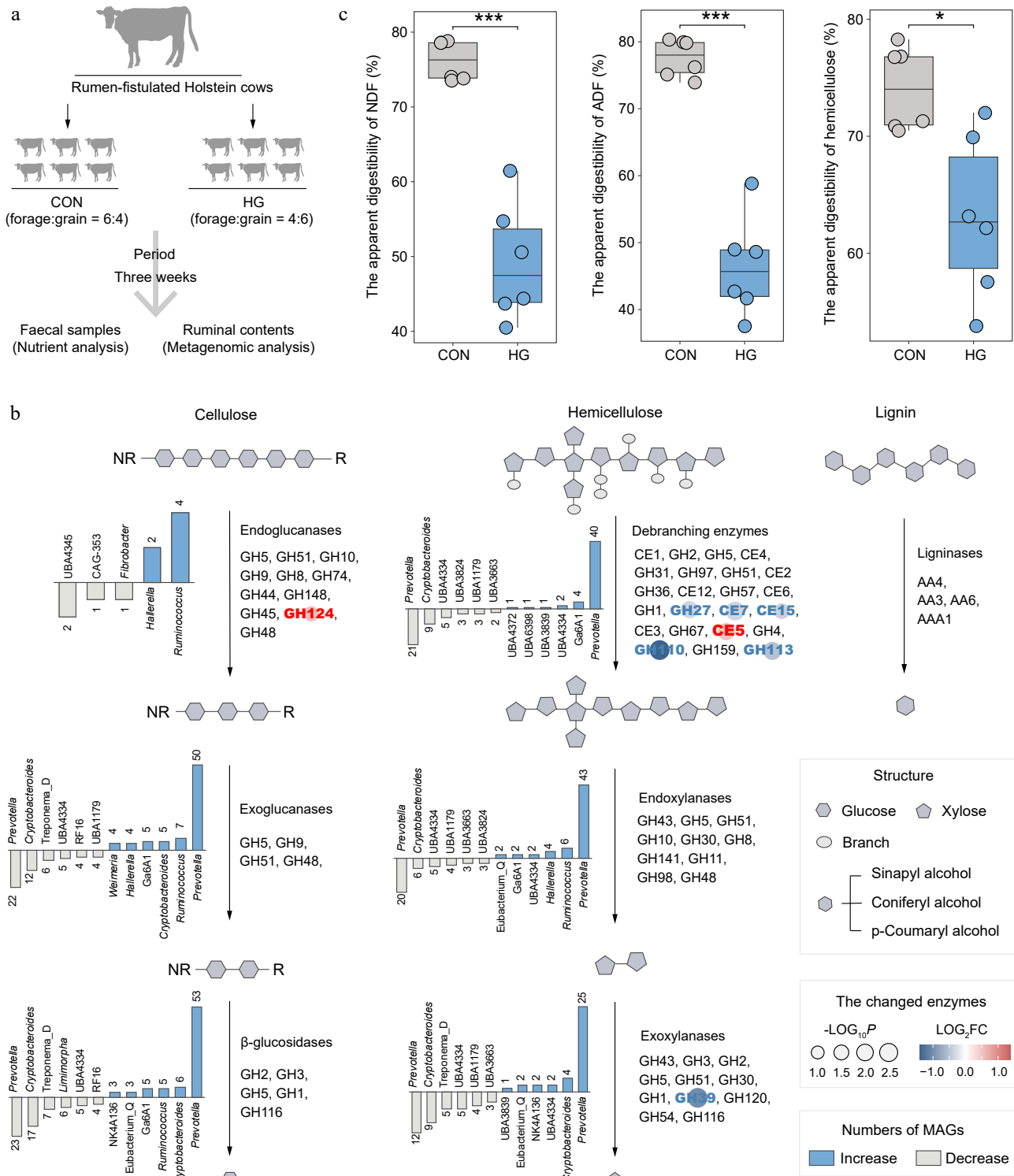


Fig. 4 Alterations in the lignocellulose degradation potential of rumen microbiota between the CON and HG groups in dairy cattle. (a) Experimental scheme of high-grain diet intervention. (b) The number and top taxonomic populations of the significantly increased and decreased abundances of lignocellulosytic microbiome (LM-MAGs) during the degradation of various lignocellulosic components in the rumen in the HG group, compared with the CON group (Wilcoxon rank-sum test, $p < 0.05$). The bar chart illustrates the number of genomes classified into specific genera with significantly different abundances, containing at least half of the CAZyme families encoding the same type of enzyme. (c) Comparison of the apparent digestibility in neutral detergent fiber (NDF), acid detergent fiber (ADF), and hemicellulose between the CON and HG groups, respectively. Significance is based on the relative index of each cohort according to the t -test. * $p < 0.05$, ** $p < 0.01$, *** $p < 0.001$.

process, a noteworthy shift transpired in the majority of *Prevotella*-affiliated genomes encoding exoglucanases and β -glucosidases under high-grain diet feeding conditions, notably marked by the decreased abundance in *Prevotella ruminicola* (Supplementary Table S8).

In the depolymerization process of hemicelluloses, it is notable that the high-grain diet significantly decreased the abundance of various debranching enzymes, including acetylxylan esterases (CE7 and CE15), α -galactosidases (GH27 and GH110), and mannosidase

(GH113) (Fig. 4b). Furthermore, a subsequent decline in the abundance of exoxyanases GH39 was observed after feeding the high-grain diets (Fig. 4b), leading to the inhibition of debranching activity in hemicellulose and subsequent degradation of xylan chains. This reduction was primarily attributed to a substantial decrease in the abundance of *Prevotella*-affiliated genomes (Fig. 4b). However, enzymes involved in lignin modification and degradation processes exhibited no significant changes after high-grain diet feeding.

As expected, nutrient content analysis of fecal samples revealed a significant reduction in the apparent digestibility of neutral detergent fiber (NDF) and acid detergent fiber (ADF) in response to the high-grain diet (t -test, $p < 0.001$; Fig. 4c). In addition, the high-grain diet significantly decreased the apparent digestibility of hemicellulose ($p = 0.01$). Therefore, the high-grain diet reduces the degradation of lignocellulose, primarily manifested in its impact on the degradation of hemicellulose.

The critical stages affected by high-grain diets in the lignocellulolytic cascades

To gain a deeper understanding of the specific stage of lignocellulose degradation affected by high-grain diets, resulting in an overall decrease in digestibility, the study was extended to encompass a more extensive temporal dimension. *Leymus chinensis* was subjected to incubation within the rumens of the six fistulated cows, comprising three forage-fed and three grain-fed cows, over 36 h (Fig. 5a). The samples were taken at nine different time points (0, 0.5, 2, 4, 6, 8, 12, 24, and 36 h) for nutrient analysis, 16S rRNA gene sequencing, and metagenomics (Fig. 5a). Nutrient analysis revealed a decrease in the digestibility of NDF, cellulose, and hemicellulose of *leymus chinensis* during *in situ* rumen later-stage incubation, especially at 36 h (t -test, $p < 0.05$; Fig. 5b). It is noteworthy that high-grain diets significantly impacted hemicellulose degradation during the initial phase of rumen incubation, resulting in reduced digestibility at 0.5 h and 2 h (t -test, $p < 0.05$; Fig. 5b). However, the digestibility of cellulose during the early stage of rumen incubation was unaffected by high-grain diets (t -test, $p < 0.05$; Fig. 5b). Therefore, the effect of high-grain diets on the degradation of hemicellulose during the initial stage of rumen incubation emerges as a crucial factor contributing to the overall reduction in lignocellulose degradation.

To understand the effect of high-grain diets on microbial colonization trajectories, fiber-adherent 16S rRNA gene sequencing data was analyzed at the amplicon sequence variant (ASV) level. The ordination analysis revealed a distinct distribution between the CON and HG groups ($p = 0.0001$, ANOSIM 9999 permutations; Fig. 5c). Considering the variable 'timepoint' showed that microbial taxa in the CON group exhibited a clear separation over time, indicating a regular colonization pattern following the degradation process (Fig. 5d). In contrast, the high-grain diet disrupted the colonization pattern of microorganisms, resulting in a mixing of microbiota at different time points (Fig. 5e). It was speculated that the high-grain diet affects the initial stage of the degradation period, resulting in no separation of microbial colonization in different degradation periods. Moreover, the diversity curve showed that alpha diversity (richness and evenness) in the HG group was lower than that in the CON group from 0.5 h during the rumen incubation (Fig. 5f, g).

Indicator species and edge analysis were conducted to identify 786 ASVs with significantly changed abundance during rumen incubation under grain introduction, mainly belonging to *Prevotella* (120 ASVs), *Rikenellaceae RC9 gut group* (72 ASVs), Unclassified F082 (59 ASVs), *Christensenellaceae R-7 group* (57 ASVs), and *Ruminococcus* (39 ASVs) (indicator species: $p < 0.05$ and edgeR: FDR < 0.05 ; Supplementary Table S9). These diet-sensitive 786 ASVs were further clustered into 18 dominant co-occurrence modules using weighted correlation network analysis (WGCNA) among eight time points during the rumen

incubation (Fig. 5h). Specifically, the ASVs from modules 1, 8, and 10 significantly decreased in abundance at different time points under the high-grain diet conditions (Fig. 5i). The ASVs from module 1 belonged to the *Rikenellaceae RC9 gut group* and showed a notable decline in abundance during the later stages (12–36 h) of rumen incubation under high-grain diet conditions (Supplementary Table S9). The ASVs from module 10 belonged to *Treponema* and *Fibrobacter* also demonstrated a substantial reduction in abundance during the later stages (12–36 h) of rumen incubation under high-grain diet conditions (Supplementary Table S9). Furthermore, ASVs from module 8, predominantly attributed to *Prevotella* (70.97%), exhibited a significant decrease in abundance during the early stages (0.5–8 h) of rumen incubation under high-grain diet conditions (Supplementary Table S9). This implies that *Prevotella* spp. may play a pivotal role as a key executor in the reduction of early-stage hemicellulose degradation.

The 1353 LM-MAGs were further utilized as a genomic database to analyze the metagenomic data from fiber-adherent samples and found that 740 LM-MAGs colonized *leymus chinensis* during rumen incubation (TPM > 0), with the majority (about 19.6%) belonging into *Prevotella* (Supplementary Table S10). Notably, a decrease in the abundance of *Prevotella*-affiliated MAGs were observed in the HG-fed cow rumen, which was most significant from 0.5 to 8 h of rumen incubation compared to the CON group (Supplementary Fig. S2). This phenomenon reiterated the initial 16S rRNA gene observations. In detail, MAG168, MAG160, MAG421, MAG1102, MAG646, MAG1207, and MAG763 mainly colonized from 0.5 to 8 h of rumen incubation in the CON group, while their colonization abundance was much lower in the HG group. Additionally, *Prevotella ruminicola* (MAG71, MAG1076, and MAG906) and *Prevotella sp900100635* (MAG170 and MAG413) mainly colonized at 8 h of rumen incubation in the CON group. These *Prevotella* spp. showed a strong potential for hemicellulose degradation, as inferred from the enrichment family GH43 (Supplementary Table S4). The present genome-centric analysis further supports the hypothesis that the high-grain diet affects the degradation of amorphous regions in lignocellulose during the initial stage of rumen incubation. This effect was largely dependent on the *Prevotella*-dominated reduction in hemicellulose degradation.

Discussion

Despite the impressive ability of rumen microbiota in dairy cattle to convert low-quality lignocellulose into nutrient-rich milk, approximately 50% of plant biomass is still resistant to degradation^[53]. Previous studies have explored carbohydrate-degrading enzyme libraries within the rumen microbiomes of dairy cattle^[46]. However, the limited number of dairy cattle has hindered our understanding of the microbial mechanisms involved in the degradation cascades of lignocellulose. In this study, all publicly available rumen metagenomes of dairy cattle were compiled and supplemented them with our own data, creating a comprehensive dataset to elucidate 1353 high-quality microbial genomes involved in lignocellulose degradation in the rumen. The present study provided a systematic description of these 1353 high-quality LM-MAGs spanning 23 phyla, representing a crucial foundation for a comprehensive understanding of rumen lignocellulose degradation efficiency in dairy cattle and creating opportunities for further improvement.

Given the diversity and redundancy of lignocellulolytic CAZymes, it was observed that different microbial consortia employed distinct enzymatic strategies in the degradation cascades of specific lignocellulosic components, including cellulose, hemicellulose, and lignin. Cellulose, the main component of lignocellulose, is degraded through the synergistic action of three classes of enzymes, including endoglucanases, exoglucanases, and β -glucosidases^[54–56]. Members of *Fibrobacter* and *Ruminococcus* (e.g., *Ruminococcus flavefaciens*) were

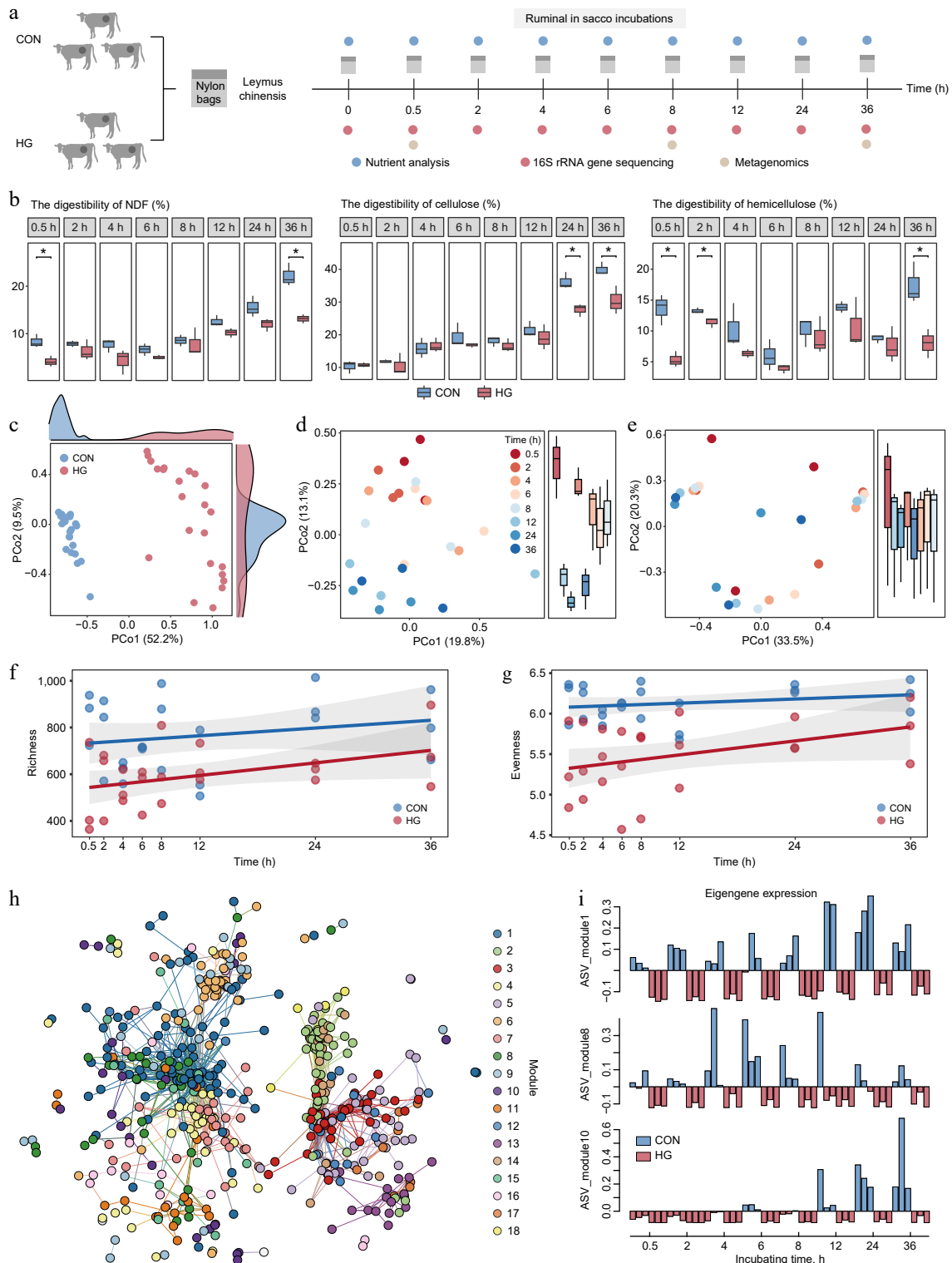


Fig. 5 Key stages of reduction in lignocellulose degradation with high-grain diet intervention. (a) Experimental scheme of rumen *in situ* incubations. (b) Comparison of digestibility in neutral detergent fiber (NDF), cellulose, and hemicellulose of incubated *Leymus chinensis* materials at each time point between the CON and HG groups according to the *t*-test, respectively. * $p < 0.05$, ** $p < 0.01$, *** $p < 0.001$. (c) Principal Coordinate Analysis (PCoA) plot generated from Bray-Curtis dissimilarity matrices using *Leymus chinensis*-adherent ASV abundances during rumen incubation in both the CON and HG groups. (d) Principal Coordinate Analysis (PCoA) plot generated from Bray-Curtis dissimilarity matrices using *Leymus chinensis*-adherent ASV abundances at 0.5, 2, 4, 6, 8, 12, 24, and 36 h during rumen incubation in the CON group. (e) Principal Coordinate Analysis (PCoA) plot generated from Bray-Curtis dissimilarity matrices using *Leymus chinensis*-adherent ASV abundances at 0.5, 2, 4, 6, 8, 12, 24, and 36 h during rumen incubation in the HG group. Temporal shift of richness ((f), Observed number of ASVs) and evenness ((g), Shannon diversity) indexes of ASVs between the CON and HG groups, respectively. (h) The co-occurrence network visualizing significant correlations of diet-sensitive 786 ASVs among eight time points during the rumen incubation ($R > 0.7$). (i) Eigengene expression of module 1, module 8, and module 10 in the CON and HG groups. CON, high-forage diet; HG, high-grain diet; ASV, amplicon sequence variants.

predicted as powerful degraders to process endo- and exoglucanases to target amorphous and crystalline cellulose^[57]. An interesting phenomenon was the striking enrichment of non-catalytic domain CBMs in genera *Fibrobacter* and *Ruminococcus*. It was found that *Fibrobacter* spp. contained tandemly arranged CBM families anchored to cellulosic biomass. The absence of CBMs leads to a significant reduction in the binding affinity and enzymatic activity of enzyme proteins towards crystalline cellulose^[58]. In contrast, the substrate adhesion effects of multiple CBMs can greatly promote the enzymatic activities of the catalytic domains of CAZymes^[13,59]. Therefore, the presence of multiple CBMs-harboring GH domains in *Fibrobacter* spp. in cow rumen is more advantageous for cellulases to attach to the hydrophobic surface of the crystalline substrate, thereby enhancing the degradation processivity. Compared to cellulose-degrading taxa, the main players in hemicellulose degradation, *Prevotella* spp. and *Cryptobacteroides* spp., had relatively fewer CBM domains but encoded numerous PULs to degrade the main and side chains of hemicellulose^[14]. The enrichment of acetylxytan esterase-contained PULs contributes largely to hemicellulose degradation. A significant proportion of the xylose residues in hemicellulose are estimated to be substituted with acetyl groups at the O-2 or O-3 position, ranging from approximately 22% to 50%^[60]. The acetylxytan esterase encoded by *Prevotella* spp. and *Cryptobacteroides* spp. can remove these acetyl groups of hemicellulose to improve the degradation efficiency of other enzymes. Therefore, the different bacterial consortia employed diverse enzymatic strategies for degradation cascades of various lignocellulosic components.

Previous studies have shown that feeding high-grain diets impacts the ability of ruminal microbes to degrade fiber^[4,61]. The present findings further suggest that a high-grain diet specifically disrupts the degradation cascade of hemicellulose. This was evident in the significant decrease of acetylxytan esterases (CE7 and CE15), α -galactosidases (GH27 and GH110), mannosidases (GH113), and exoxylanases (GH39) under high-grain diet conditions, which leads to a decrease in debranching activity in hemicellulose and subsequent degradation of xylan chains. Notably, this process was primarily driven by the reduction of *Prevotella* spp. The decreased apparent digestibility of hemicellulose under high-grain diet conditions supported this phenomenon. Through further extending the present study to multiple time points, it was discovered that a high-grain diet decreased the early-stage degradation of hemicellulose by *Prevotella* spp., leading to the reduced degradation of the amorphous regions of lignocellulose. This reduction in turn reduces the accessibility of microbial degrading enzymes to the ordered crystalline cellulose and results in ineffective degradation of lignocellulose^[12]. The present results showed that feeding high-grain diets disrupted the ordered colonization of microorganisms on *Leymus chinensis*, resulting in the non-separation of microbiota at different colonization time points. Therefore, the *Prevotella*-dominated reduction in hemicellulose degradation during the initial stage of rumen incubation may be the primary reason for the reduced digestibility of lignocellulose under high-grain diet feeding.

In addition, it was found that some lignocellulose-degrading bacteria were significantly enriched under high-grain conditions, and importantly, they belong to microbial taxa that have not been described before in ruminants. For example, *Hallerella* spp., the nearest phylogenetic neighbor of *Fibrobacter* spp.^[52], were found to possess a large amount of endoglucanases and exoglucanases. *Hallerella*-affiliated MAGs were found to only attach to fiber in cows fed high-grain diets, indicating their important role in lignocellulose degradation in such environments. Despite both belonging to the Fibrobacteraceae family, *Fibrobacter* spp. and *Hallerella* spp. had different adaptabilities in various environments. In detail, *Fibrobacter* was more suitable for

high-fiber environments, while *Hallerella* exhibited fiber degradation ability in low-fiber environments. Additionally, members of *Sodaliophilus* were predicted to possess the capability of lignocellulose degradation through extracellular enzymes or polysaccharide utilization loci (PULs), and their abundance exhibited a significant increase under high-grain diet conditions. Previous studies have shown that high-grain diets can lead to a decrease in the abundance of lignocellulose-degrading microorganisms^[4,62]. Therefore, these newly discovered potential lignocellulose-degrading bacteria in the rumen of dairy cattle represent important resources for development. These bacteria could help mitigate the reduced lignocellulose degradation capacity associated with high-grain feeding. Although further research is needed to confirm the actual lignocellulose degradation capabilities of these microorganisms, our findings provide valuable support for future efforts aimed at enhancing the degradation efficiency of lignocellulose in the rumen of dairy cattle fed high-grain diets.

In addition to bacteria, several studies have explored the genomes of eukaryotic organisms, such as fungi and ciliates, in the rumen^[63,64]. These studies have revealed that these organisms encode a variety of carbohydrate-related genes and enzymes, showing their significant capabilities for degrading plant fiber. The present study primarily focuses on prokaryotic genomic research related to the microbial degradation of rumen carbohydrates. Future research should clarify how high-grain diets influence different lignocellulosic components and the various stages of lignocellulolytic cascades through specific protozoa and fungi. This will contribute to a more comprehensive understanding of the role of rumen microorganisms in carbohydrate degradation.

Conclusions

The present study utilized a genome-centric approach to identify 1353 high-quality MAGs involved in lignocellulose degradation in the cow rumen. By analyzing their enzymatic strategies for different substrate types, insights into the complexity and specialization of ruminal microbial populations in degrading various lignocellulosic components were gained, with a particular emphasis on cellulose and hemicellulose degradation, while highlighting their limited role in lignin degradation. Through spatial and temporal studies involving diet interventions and rumen *in situ* incubation, it was discovered that a high-grain diet primarily interfered with the degradation of amorphous regions of lignocellulose and significantly reduced hemicellulose degradation by *Prevotella*-dominated communities. These findings underscore the intricate interplay among diet, microbial consortia, and enzymatic strategies in the rumen, highlighting the potential for manipulating the rumen microbiota to improve the efficiency of lignocellulose degradation in dairy cattle.

Ethical statement

All procedures were reviewed and preapproved by the the Nanjing Agricultural University Institutional Animal Care and Use Committee, identification number: SYXK-2017-0027, approval date: 2019-3-12. The research followed the 'Replacement, Reduction, and Refinement' principles to minimize harm to animals. This article provides details on the housing conditions, care, and pain management for the animals, ensuring that the impact on the animals is minimized during the experiment.

Author contributions

The authors confirm contribution to the paper as follows: study conception and design: Mao S, Zhu W; samples collection and

experiments conduction: Lin L, Yang H, Zhang Jiyou, Lai Z, Qi W, Ma H, Zhang Jiawei; published rumen metagenome collection: Xie F, Lin L; bioinformatic analyses, data visualization and interpretation, draft manuscript preparation: Lin L; manuscript revision: Mao S. All authors read, edited, and approved the final manuscript.

Data availability

Raw sequence reads for all 18 incubated *leymus chinensis* samples are available under European Nucleotide Archive (ENA) project PRJNA955930. All MAGs produced and utilized in this study have been deposited in Figshare (<https://figshare.com/s/dcaad3555e232551029>). The data sources for an additional 226 published ruminal metagenome samples from dairy cattle are provided in [Supplementary Table S1](#). Please note that although there were 48 samples available under PRJNA214227 as reported by Wolff et al.^[27], we exclusively utilized 16 rumen samples from dairy cattle. For other projects, we also exclusively utilized rumen samples from dairy cattle.

Acknowledgments

The current project was supported by the high-performance computing platform of Bioinformatics Center, Nanjing Agricultural University. This research was funded by the National Key R&D Program of China (2022YFD1301001).

Conflict of interest

The authors declare that they have no conflict of interest. Shengyong Mao is the Editorial Board member of *Animal Advances* who was blinded from reviewing or making decisions on the manuscript. The article was subject to the journal's standard procedures, with peer-review handled independently of this Editorial Board member and the research groups.

Supplementary information accompanies this paper at (<https://www.maxapress.com/article/doi/10.48130/animadv-0024-0002>)

References

- Johansen KS. 2016. Lytic polysaccharide monoxygenases: the microbial power tool for lignocellulose degradation. *Trends in Plant Science* 21:926–36
- Shahab RL, Brethauer S, Davey MP, Smith AG, Vignolini S, et al. 2020. A heterogeneous microbial consortium producing short-chain fatty acids from lignocellulose. *Science* 369:eabb1214
- King AJ, Cragg SM, Li Y, Dymond J, Guille MJ, et al. 2010. Molecular insight into lignocellulose digestion by a marine isopod in the absence of gut microbes. *Proceedings of the National Academy of Sciences of the United States of America* 107:5345–50
- Lin L, Lai Z, Zhang J, Zhu W, Mao S. 2023. The gastrointestinal microbiome in dairy cattle is constrained by the deterministic driver of the region and the modified effect of diet. *Microbiome* 11:10
- Hess M, Sczyrba A, Egan R, Kim TW, Chokhwalala H, et al. 2011. Metagenomic discovery of biomass-degrading genes and genomes from cow rumen. *Science* 331:463–67
- Xie F, Jin W, Si H, Yuan Y, Tao Y, et al. 2021. An integrated gene catalog and over 10,000 metagenome-assembled genomes from the gastrointestinal microbiome of ruminants. *Microbiome* 9:137
- Artzi L, Bayer EA, Morais S. 2017. Cellulosomes: bacterial nanomachines for dismantling plant polysaccharides. *Nature Reviews Microbiology* 15:83–95
- Gharechahi J, Vahidi MF, Sharifi G, Ariaenejad S, Ding XZ, et al. 2023. Lignocellulose degradation by rumen bacterial communities: New insights from metagenome analyses. *Environmental Research* 229:115925
- Seshadri R, Leahy SC, Attwood GT, Teh KH, Lambie SC, et al. 2018. Cultivation and sequencing of rumen microbiome members from the Hungate1000 Collection. *Nature Biotechnology* 36:359–67
- Michalak L, Gaby JC, Lagos L, La Rosa SL, Hvidsten TR, et al. 2020. Microbiota-directed fibre activates both targeted and secondary metabolic shifts in the distal gut. *Nature Communications* 11:5773
- Gálvez EJC, Iljazovic A, Amend L, Lesker TR, Renault T, et al. 2020. Distinct polysaccharide utilization determines interspecies competition between intestinal *Prevotella* spp. *Cell Host & Microbe* 28:838–852.E6
- Novy V, Aissa K, Nielsen F, Straus SK, Ciesielski P, et al. 2019. Quantifying cellulose accessibility during enzyme-mediated deconstruction using 2 fluorescence-tagged carbohydrate-binding modules. *Proceedings of the National Academy of Sciences of the United States of America* 116:22545–51
- Shi Q, Abdel-Hamid AM, Sun Z, Cheng Y, Tu T, et al. 2023. Carbohydrate-binding modules facilitate the enzymatic hydrolysis of lignocellulosic biomass: Releasing reducing sugars and dissociative lignin available for producing biofuels and chemicals. *Biotechnology Advances* 65:108126
- Morais S, Mizrahi I. 2019. Islands in the stream: from individual to communal fiber degradation in the rumen ecosystem. *FEMS microbiology reviews* 43:362–79
- Gharechahi J, Vahidi MF, Ding XZ, Han JL, Salekdeh GH. 2020. Temporal changes in microbial communities attached to forages with different lignocellulosic compositions in cattle rumen. *FEMS Microbiology Ecology* 96:fiia069
- Gharechahi J, Vahidi MF, Bahram M, Han JL, Ding XZ, et al. 2021. Metagenomic analysis reveals a dynamic microbiome with diversified adaptive functions to utilize high lignocellulosic forages in the cattle rumen. *The ISME Journal* 15:1108–20
- Van Soest PJ, Robertson JB, Lewis BA. 1991. Methods for dietary fiber, neutral detergent fiber, and nonstarch polysaccharides in relation to animal nutrition. *Journal of Dairy Science* 74:3583–97
- Van Keulen J, Young BA. 1977. Evaluation of acid-insoluble ash as a natural marker in ruminant digestibility studies. *Journal of Animal Science* 44:282–87
- Yu Z, Morrison M. 2004. Improved extraction of PCR-quality community DNA from digesta and fecal samples. *Biotechniques* 36:808–12
- Magoč T, Salzberg SL. 2011. FLASH: fast length adjustment of short reads to improve genome assemblies. *Bioinformatics* 27:2957–63
- Callahan BJ, McMurdie PJ, Han AW, Johnson AJA, et al. 2016. DADA2: High-resolution sample inference from Illumina amplicon data. *Nature Methods* 13:581–83
- Bolyen E, Rideout JR, Dillon MR, Bokulich NA, Abnet CC, et al. 2019. Reproducible, interactive, scalable and extensible microbiome data science using QIIME 2. *Nature Biotechnology* 37:852–57
- Quast C, Pruesse E, Yilmaz P, Gerken J, Schweer T, et al. 2013. The SILVA ribosomal RNA gene database project: improved data processing and web-based tools. *Nucleic Acids Research* 41:D590–D596
- Bokulich NA, Kaehler BD, Rideout JR, Dillon M, Bolyen E, et al. 2018. Optimizing taxonomic classification of marker-gene amplicon sequences with QIIME 2's q2-feature-classifier plugin. *Microbiome* 6:90
- Li J, Zhong H, Ramayo-Caldas Y, Terrapon N, Lombard V, et al. 2020. A catalog of microbial genes from the bovine rumen unveils a specialized and diverse biomass-degrading environment. *Gigascience* 9:giaa057
- Glendinning L, Genç B, Wallace RJ, Watson M. 2021. Metagenomic analysis of the cow, sheep, reindeer and red deer rumen. *Scientific reports* 11:1990
- Wolff SM, Ellison MJ, Hao Y, Cockrum RR, Austin KJ, et al. 2017. Diet shifts provoke complex and variable changes in the metabolic networks of the ruminal microbiome. *Microbiome* 5:60
- Li W, Han Y, Yuan X, Wang G, Wang Z, et al. 2017. Metagenomic analysis reveals the influences of milk containing antibiotics on the rumen microbes of calves. *Archives of Microbiology* 199:433–43
- Wang L, Zhang G, Xu H, Xin H, Zhang Y. 2019. Metagenomic analyses of microbial and carbohydrate-active enzymes in the rumen of holstein cows fed different forage-to-concentrate ratios. *Frontiers in Microbiology* 10:649
- Xue MY, Sun HZ, Wu XH, Liu JX, Guan LL. 2020. Multi-omics reveals that the rumen microbiome and its metabolome together with the host metabolome contribute to individualized dairy cow performance. *Microbiome* 8:64
- Xue MY, Xie YY, Zhong Y, Ma XJ, Sun HZ, et al. 2022. Integrated meta-omics reveals new ruminal microbial features associated with feed efficiency in dairy cattle. *Microbiome* 10:32

32. Mu YY, Qi WP, Zhang T, Zhang JY, Mao SY. 2021. Gene function adjustment for carbohydrate metabolism and enrichment of rumen microbiota with antibiotic resistance genes during subacute rumen acidosis induced by a high-grain diet in lactating dairy cows. *Journal of Dairy Science* 104:2087–105
33. Wu X, Huang S, Huang J, Peng P, Liu Y, et al. 2021. Identification of the potential role of the rumen microbiome in milk protein and fat synthesis in dairy cows using metagenomic sequencing. *Animals* 11:1247
34. Chen S, Zhou Y, Chen Y, Gu J. 2018. fastp: an ultra-fast all-in-one FASTQ preprocessor. *Bioinformatics* 34:i884–i890
35. Kang DD, Froula J, Egan R, Wang Z. 2015. MetaBAT, an efficient tool for accurately reconstructing single genomes from complex microbial communities. *PeerJ* 3:e1165
36. Li D, Liu CM, Luo R, Sadakane K, Lam TW. 2015. MEGAHIT: an ultra-fast single-node solution for large and complex metagenomics assembly via succinct de Bruijn graph. *Bioinformatics* 31:1674–76
37. Wu YW, Simmons BA, Singer SW. 2016. MaxBin 2.0: an automated binning algorithm to recover genomes from multiple metagenomic datasets. *Bioinformatics* 32:605–7
38. Alneberg J, Bjarnason BS, De Bruijn I, Schirmer M, Quick J, et al. 2014. Binning metagenomic contigs by coverage and composition. *Nature Methods* 11:1144–46
39. Uritskiy GV, DiRuggiero J, Taylor J. 2018. MetaWRAP – a flexible pipeline for genome-resolved metagenomic data analysis. *Microbiome* 6:158
40. Parks DH, Imelfort M, Skennerton CT, Hugenholtz P, Tyson GW. 2015. CheckM: assessing the quality of microbial genomes recovered from isolates, single cells, and metagenomes. *Genome Research* 25:1043–55
41. Olm MR, Brown CT, Brooks B, Banfield JF. 2017. dRep: a tool for fast and accurate genomic comparisons that enables improved genome recovery from metagenomes through de-replication. *The ISME Journal* 11:2864–68
42. Seemann T. 2014. Prokka: rapid prokaryotic genome annotation. *Bioinformatics* 30:2068–69
43. Nayfach S, Shi ZJ, Seshadri R, Pollard KS, Kyrpides NC. 2019. New insights from uncultivated genomes of the global human gut microbiome. *Nature* 568:505–10
44. Parks DH, Chuvochina M, Waite DW, Rinke C, Skarshewski A, et al. 2018. A standardized bacterial taxonomy based on genome phylogeny substantially revises the tree of life. *Nature Biotechnology* 36:996
45. Segata N, Börnigen D, Morgan XC, Huttenhower C. 2013. PhyloPhlAn is a new method for improved phylogenetic and taxonomic placement of microbes. *Nature Communications* 4:2304
46. Letunic I, Bork P. 2016. Interactive tree of life (iTOL) v3: an online tool for the display and annotation of phylogenetic and other trees. *Nucleic Acids Research* 44:W242–W245
47. Zhang H, Yohe T, Huang L, Entwistle S, Wu P, et al. 2018. dbCAN2: a meta server for automated carbohydrate-active enzyme annotation. *Nucleic Acids Research* 46:W95–W101
48. Potter SC, Luciani A, Eddy SR, Park Y, Lopez R, et al. 2018. HMMER web server: 2018 update. *Nucleic Acids Research* 46:W200–W204
49. Lombard V, Golaconda Ramulu H, Drula E, Coutinho PM, Henrissat B. 2014. The carbohydrate-active enzymes database (CAZy) in 2013. *Nucleic Acids Research* 42:D490–D495
50. Stewart RD, Auffret MD, Roehe R, Watson M. 2018. Open prediction of polysaccharide utilisation loci (PUL) in 5414 public *Bacteroidetes* genomes using PULpy. *bioRxiv* Preprint:421024
51. Yeoman CJ, Fields CJ, Lepercq P, Ruiz P, Forano E, et al. 2021. *In Vivo* competitions between *Fibrobacter succinogenes*, *Ruminococcus flavefaciens*, and *Ruminococcus albus* in a gnotobiotic sheep model revealed by multi-omic analyses. *mBio* 12:e03533–20
52. Wylensek D, Hitch TCA, Riedel T, Afrizal A, Kumar N, et al. 2020. A collection of bacterial isolates from the pig intestine reveals functional and taxonomic diversity. *Nature Communications* 11:6389
53. Terry SA, Badhan A, Wang Y, Chaves AV, McAllister TA. 2019. Fibre digestion by rumen microbiota—a review of recent metagenomic and metatranscriptomic studies. *Canadian Journal of Animal Science* 99:678–92
54. Wang K, Gao P, Geng L, Liu C, Zhang J, et al. 2022. Lignocellulose degradation in *Protaetia brevitarsis* larvae digestive tract: refining on a tightly designed microbial fermentation production line. *Microbiome* 10:90
55. Hagen LH, Brooke CG, Shaw CA, Norbeck AD, Piao H, et al. 2021. Proteome specialization of anaerobic fungi during ruminal degradation of recalcitrant plant fiber. *The ISME Journal* 15:421–34
56. Cabral L, Persinoti GF, Paixão DAA, Martins MP, Morais MAB, et al. 2022. Gut microbiome of the largest living rodent harbors unprecedented enzymatic systems to degrade plant polysaccharides. *Nature Communications* 13:629
57. Froidurot A, Julliard V. 2022. Cellulolytic bacteria in the large intestine of mammals. *Gut Microbes* 14:2031694
58. Beckham GT, Matthews JF, Peters B, Bomble YJ, Himmel ME, et al. 2011. Molecular-level origins of biomass recalcitrance: decrystallization free energies for four common cellulose polymorphs. *The Journal of Physical Chemistry B* 115:4118–27
59. Zhang KD, Li W, Wang YF, Zheng YL, Tan FC, et al. 2018. Processive degradation of crystalline cellulose by a multimodular endoglucanase via a wirewalking mode. *Biomacromolecules* 19:1686–96
60. Ding S, Cao J, Zhou R, Zheng F. 2007. Molecular cloning, and characterization of a modular acetyl xylan esterase from the edible straw mushroom *Volvariella volvacea*. *FEMS Microbiology Letters* 274:304–10
61. Rivera-Chacon R, Pacifico C, Ricci S, Petri RM, Reisinger N, et al. 2024. Prolonged feeding of high-concentrate diet remodels the hindgut microbiome and modulates nutrient degradation in the rumen and the total gastrointestinal tract of cows. *Journal of Dairy Science* In Press
62. Xie F, Xu L, Wang Y, Mao S. 2021. Metagenomic sequencing reveals that high-grain feeding alters the composition and metabolism of cecal microbiota and induces cecal mucosal injury in sheep. *mSystems* 6:e00915–21
63. Li Z, Wang X, Zhang Y, Yu Z, Zhang T, et al. 2022. Genomic insights into the phylogeny and biomass-degrading enzymes of rumen ciliates. *The ISME Journal* 16:2775–87
64. Peng X, Wilken SE, Lankiewicz TS, Gilmore SP, Brown JL, et al. 2021. Genomic and functional analyses of fungal and bacterial consortia that enable lignocellulose breakdown in goat gut microbiomes. *Nature Microbiology* 6:499–511



Copyright: © 2024 by the author(s). Published by Maximum Academic Press on behalf of Nanjing Agricultural University. This article is an open access article distributed under Creative Commons Attribution License (CC BY 4.0), visit <https://creativecommons.org/licenses/by/4.0/>.